Oecologia (2005) 143: 337–348
DOI 10.1007/s00442-004-1813-y

METHODS

Gabriel J. Bowen · Leonard I. Wassenaar
Keith A. Hobson

Global application of stable hydrogen and oxygen isotopes to wildlife forensics

Received: 25 June 2004 / Accepted: 15 December 2004 / Published online: 23 February 2005

Abstract Stable isotopes are being increasingly used in wildlife forensics as means of determining the origin and movement of animals. The heavy isotope content of precipitated water and snow (δD_p, $\delta^{18}O_p$) varies widely and systematically across the globe, providing a label that is incorporated through diet into animal tissue. As a result, these isotopes are potentially ideal tracers of geographic origin. The hydrogen and oxygen isotope tracer method has excellent potential where (1) spatial variation of precipitation isotopes exist, and (2) strong, mechanistic relationships link precipitation and isotope ratios in biological tissue. Here, we present a method for interpolation of precipitation isotope values and use it to create global basemaps of growing-season (GS) and mean annual (MA) δD_p and $\delta^{18}O_p$. The use of these maps for forensic application is demonstrated using previously published isotope data for bird feathers (δD_f) in North America and Europe. The precipitation maps show that the greatest potential for applying hydrogen and oxygen isotope forensics exists in mid- to high-latitude continental regions, where strong spatial isotope gradients exist. We demonstrate that $\delta D_f/\delta D_p$ relationships have significant predictive power both in North America and Europe, and show how zones of confidence for the assignment of origin can be described using these predictive relationships. Our analysis focuses on wildlife forensics, but the maps and approaches presented here will be equally applicable to criminal forensic studies involving biological materials. These maps are available in GIS format at http://www.waterisotopes.org.

Keywords Stable isotopes · Deuterium · Oxygen-18 · Precipitation · Migration · Forensics

G. J. Bowen (✉)
Department of Biology, University of Utah,
257 South 1400 East, Salt Lake City, UT 84112, USA
E-mail: gbowen@biology.utah.edu
Tel.: +1-801-5850415
Fax: +1-801-5814665

L. I. Wassenaar
National Water Research Institute,
Environment Canada, 11 Innovation Blvd, Saskatoon,
S7N 3H5, SK,Canada

K. A. Hobson
Environment Canada, Canadian Wildlife Service,
115 Perimeter Road, Saskatoon,
S7N 0X4, SK, Canada

Introduction

The use of stable isotopes in wildlife environmental forensics is a new and rapidly developing field that has seen tremendous growth in the past decade (Rubenstein and Hobson 2004). This new approach exploits the fact that the ratio of naturally occurring light stable isotopes (D/H, $^{13}C/^{12}C$, $^{15}N/^{14}N$, $^{34}S/^{32}S$) in dietary items may vary predictably among biomes, which organisms inhabit. The overall isotopic makeup of individuals in food webs of a particular biome is controlled by a number of complicated and inter-related environmental factors, including climate, altitude, geological and soil composition, food chain length, tissue turnover and the individual's residency time. More specifically, the isotopic composition of a specific animal tissue is controlled mainly by local dietary inputs, although various tissues integrate local diet over different temporal scales (Hobson 1999). For example, whole blood and muscle have dynamic turnover times of days to weeks (e.g., Evans-Ogden et al. 2004; Ayliffe et al. 2004), whereas bone collagen averages the individual's lifetime of dietary inputs (Hobson and Clark 1992). Other tissues are biochemically inert following synthesis, and hence may reflect local diet over a very short time period (e.g., feathers) or record temporal dietary time sequences (e.g., hair, tusk, nails). As organisms live in or move between isotopically distinct biomes, they record isotope signatures that provide means for reconstruction of their origins or movements. The fundamental premise of this application has been clearly validated, and the stage is

set for the increasingly widespread use of stable isotope tracking in environmental (e.g., migratory connectivity) and criminal (e.g., illegal animal trade, animal origin) forensics.

Stable isotope forensics has proven very successful in studies of migratory connectivity over large geospatial scales. Examples include stable carbon, sulfur and hydrogen isotope studies of migrant birds and insects whose summering and wintering grounds are separated by thousands of kilometers (e.g., Chamberlain et al. 1997; Hobson and Wassenaar 1997; Wassenaar and Hobson 1998; Rubenstein et al. 2002). Keen interest in migratory connectivity is driven by the need to better understand migratory behavior and the response of migrant populations to habitat loss throughout their range (Webster et al. 2001; Rubenstein et al. 2002; Norris et al. 2003; Rubenstein and Hobson 2004). The development of effective and routinely applicable methods for tracking migratory animals across continents and hemispheres has proven difficult. Traditional methods, such as mark/recapture have proven to be largely ineffective (Hobson 2003), bringing about the need for new methods that do not require recapturing of individuals. Stable isotope methods meet this criterion, and compare favorably to other developed methods, such as satellite tracking, in that the sampling requirements are relatively non-invasive and the analytical costs involved can be quite low. However, before isotope forensics can be routinely adopted in migration studies, the geospatial distribution of the underlying environmental isotopes and the processes linking local isotope labels to animal tissues must be understood.

Currently, the most effective and well-established stable isotope environmental forensic tracer involves the measurement of hydrogen isotopes in seasonally-grown tissues such as feathers, hair and nails (Hobson 2003; Rubenstein and Hobson 2004). The hydrogen and oxygen isotope composition of environmental water varies widely and systematically across the globe (Dansgaard 1954; Craig 1961; Rozanski et al. 1993; Kendall and Coplen 2001). Because water is a key constituent of many biosynthesis reactions, the isotopic label present in local environmental water is transferred to plants and propagated through foodwebs into animal tissues (Estep and Dabrowski 1980; Hobson et al. 1999). For tissues which are biochemically inert after synthesis (e.g., keratin, bone collagen), this label may be fixed and later used to estimate the location of origin of organisms. Much of the work to date has focused on migrant birds, and the strong relationship between the hydrogen isotope values of bird feathers (δD_f) and those of GS precipitation (GS δD_p) has been demonstrated repeatedly (e.g., Chamberlain et al. 1997; Hobson and Wassenaar 1997; Meehan et al. 2001; Rubenstein et al. 2002; Hobson et al. 2004).

As the number and diversity of hydrogen isotope forensic tracer studies increases, it is critically important that the potential and limitations of the method be carefully reviewed and that guidelines for successful application be developed. The objective of this paper is to provide a critical review and evaluation of the applicability of hydrogen (and oxygen) isotope forensics at the global scale. We begin by using an informed interpolation method to create global grids of hydrogen and oxygen water isotopes for use in wildlife forensic studies. Such grids are fundamental to hydrogen and oxygen isotope forensic studies because they provide accurate point estimates for δD and $\delta^{18}O$ in precipitation that can be compared to biological and animal samples of known or unknown origin. Using the grids, we review the global distribution of hydrogen and oxygen isotopes in GS precipitation, which is likely to provide the primary hydrogen and oxygen source for many plants and foodwebs, and to investigate which regions of the globe have sufficient isotopic variation and structure to allow application of hydrogen and oxygen isotope forensics. We then build on previous studies of the isotopic composition of bird feathers to critically investigate the application of the δD_p maps to biological data sets. Using previously published feather isotope data for North American and European birds, we examine the relationships between feather and water isotopes over two continents and demonstrate a method for using the isotope grids to statistically constrain the unknown origin of individuals. The results of this work provide general guidelines for the future application of water isotopes in wildlife forensic studies involving a wide variety of biological materials. Although our discussion focuses on natural wildlife populations, many of our results apply equally to criminalistics, and in places we will point out concerns related to the application of the water isotope tracer in criminal forensic studies.

Methods

Seasonal δD and $\delta^{18}O$ precipitation maps

To construct global grids we used water isotope data from the Global Network for Isotopes in Precipitation (GNIP) database administered by the International Atomic Energy Association and World Meteorological Organization (IAEA/WMO 2001). The data available are monthly weighted average precipitation (δD_p and $\delta^{18}O_p$) values for sites on all seven continents and islands, spanning ~1960 to the present. Sampling at these sites has occurred discontinuously through time, and records for individual sites range from <1 year to decades of measurements. To derive monthly average values that best represent the δD or $\delta^{18}O$ of precipitation at a site during an 'average' year, we calculated unweighted averages for each month based on all observations throughout the period of sampling. The number of monthly average values ranged from a low of 377 for δD_p during February to a high of 418 for $\delta^{18}O_p$ during December (Fig. 1a, c).

Climatological (mean monthly temperature [t] and precipitation amount [p]) data were compiled from the

Global Historical Climatology Network (GHCN) version 2 database, administered by the WMO (Peterson and Vose 1997). These data include relatively continuous records from a large number of sites from 1800 to the present. The monitoring sites are primarily on the continents (Fig. 1e, g), and there is a strong northern hemisphere bias in the data set, but the large number of data and geographic coverage of the network is fully adequate to constrain monthly t and p values for the continental regions of interest here. We extracted observations from all sites for 1960 to the present and calculated unweighted station averages for monthly mean temperature and precipitation. This resulted in a total number of observations ranging from 4,594 to 4,600 for t and from 18,829 to 18,875 for p. To reduce the computation time required for analysis of precipitation, we resampled the p data with a regular, unweighted, one-degree averaging filter, reducing the total number of data to 6,873–6,883 (Fig. 1g).

Global grids of monthly mean δD_p and $\delta^{18}O_p$ were created using a modification of a previously described detrended interpolation method for mean annual (MA) δD_p and $\delta^{18}O_p$ (Bowen and Wilkinson 2002; Bowen and Revenaugh 2003). δD_p and $\delta^{18}O_p$ vary systematically with latitude and altitude, largely as a result of temperature-driven distillation of the heavy isotope from air masses as they move to the cooler, higher latitudes or over orographic barriers (Dansgaard 1964; Rozanski et al. 1993; Bowen and Wilkinson 2002). In addition to these general global processes, regional effects such as distillation by progressive rainout across continents and variation in the δD and $\delta^{18}O$ of water vapor sources also contributes to spatial patterns of δD_p and $\delta^{18}O_p$ (Rozanski et al. 1993; Gat et al. 1994). The detrended interpolation method expresses the predicted isotope value at a given site ($\hat{\delta}_x$) as a function of latitude and altitude parameters plus an interpolated residual term. The latitude/altitude term describes the large-scale, temperature driven variation in δD_p and $\delta^{18}O_p$, whereas the interpolated term gives an estimate of all other local or regional effects not related to temperature. The accuracy of this method was evaluated in detail by Bowen and Revenaugh (2003) and was found to significantly exceed that of other standard interpolation methods.

For MA values, the zonal symmetry of atmospheric circulation and temperature leads to a relationship between latitude and δD_p and $\delta^{18}O_p$ that is nearly symmetric about the equator, and allows the isotope data to be expressed as a simple polynomial of the absolute value of station latitude (Bowen and Wilkinson 2002). Both the distribution of temperature and the boundaries between atmospheric circulation cells move northward and southward with the seasons, however, so this symmetry is not preserved through the seasonal cycle. To allow detrending of the monthly isotope data, station latitudes must be transformed in a manner that accounts for seasonal zonal asymmetry. We explored various transformations, and found that zonal asymmetry of monthly δD_p and $\delta^{18}O_p$ values is most closely related to the seasonal precessional cycle of the intertropical convergence zone (ITCZ, Fig. 2a). This parameter is related directly to the zonal shift of the atmospheric circulation cells throughout the year, and is therefore mechanistically related to the distribution of δD_p and $\delta^{18}O_p$. By transforming stable isotope-monitoring station latitudes (lat) to effective monthly absolute latitudes (elat) by the equations:

$$\text{for lat} \geqslant \text{lat}_{\text{ITZ}}(m): \quad \text{elat} = 90\frac{\text{lat}_{\text{ITZ}}(m) - \text{lat}}{90 - \text{lat}_{\text{ITZ}}(m)} \tag{1}$$

$$\text{and for lat} < \text{lat}_{\text{ITZ}}(m): \quad \text{elat} = 90\frac{\text{lat} + \text{lat}_{\text{ITZ}}(m)}{90 + \text{lat}_{\text{ITZ}}(m)} \tag{2}$$

where $\text{lat}_{\text{ITZ}}(m)$ is the latitude of the globally averaged ITCZ for month m, estimated from the work of Waliser and Gautier (1993), the zonal asymmetry of the δD_p and $\delta^{18}O_p$ distribution is effectively removed (Fig. 2b, c).

Parameters a, b, c, and β in the nonlinear equation describing the interpolation model:

$$\hat{\delta}_x = p_x + \frac{\sum_{i=1}^{n} (\delta_i - p_i) e^{(-D_{xi}/\beta)}}{\sum_{i=1}^{n} e^{(-D_{xi}/\beta)}}, \tag{3}$$

where

$$p_x = a(\text{elat}^2) + b(\text{elat}) + c(\text{alt}), \tag{4}$$

δ_i is the measured δD_p or $\delta^{18}O_p$ value at station i, and D_{xi} is the angular distance (degrees) between gridpoint x and station i, were fitted to each monthly isotope data set using a standard gradient decent method (Bowen and Revenaugh 2003). These parameters were then applied globally on a 20′×20′ grid using land surface elevation values derived by averaging data from the 5′×5′ global ETOPO5 digital elevation model (US National Geophysical Data Center 1998). Mean monthly temperature values are latitude- and altitude-dependent in much the same way as are δD_p and $\delta^{18}O_p$, and the detrended interpolation model was also used to create 20′×20′ global t grids from the *elat*-transformed GHCN station data. Precipitation amount values, in contrast, were most closely related to regional and seasonal circulation pathways and do not exhibit robust global trends related to geographic variables such as latitude or altitude. We, therefore interpolated precipitation amount values without detrending. The 20′×20′ precipitation amount grids were created by inverse distance weighting with a spherical weighting function estimated from the empirical semivariogram of precipitation station data. Our global GS isotope grids represent a precipitation amount-weighted average of δD_p or $\delta^{18}O_p$ values for 'growing-season' months, which we define to be those months with an average temperature >0°C.

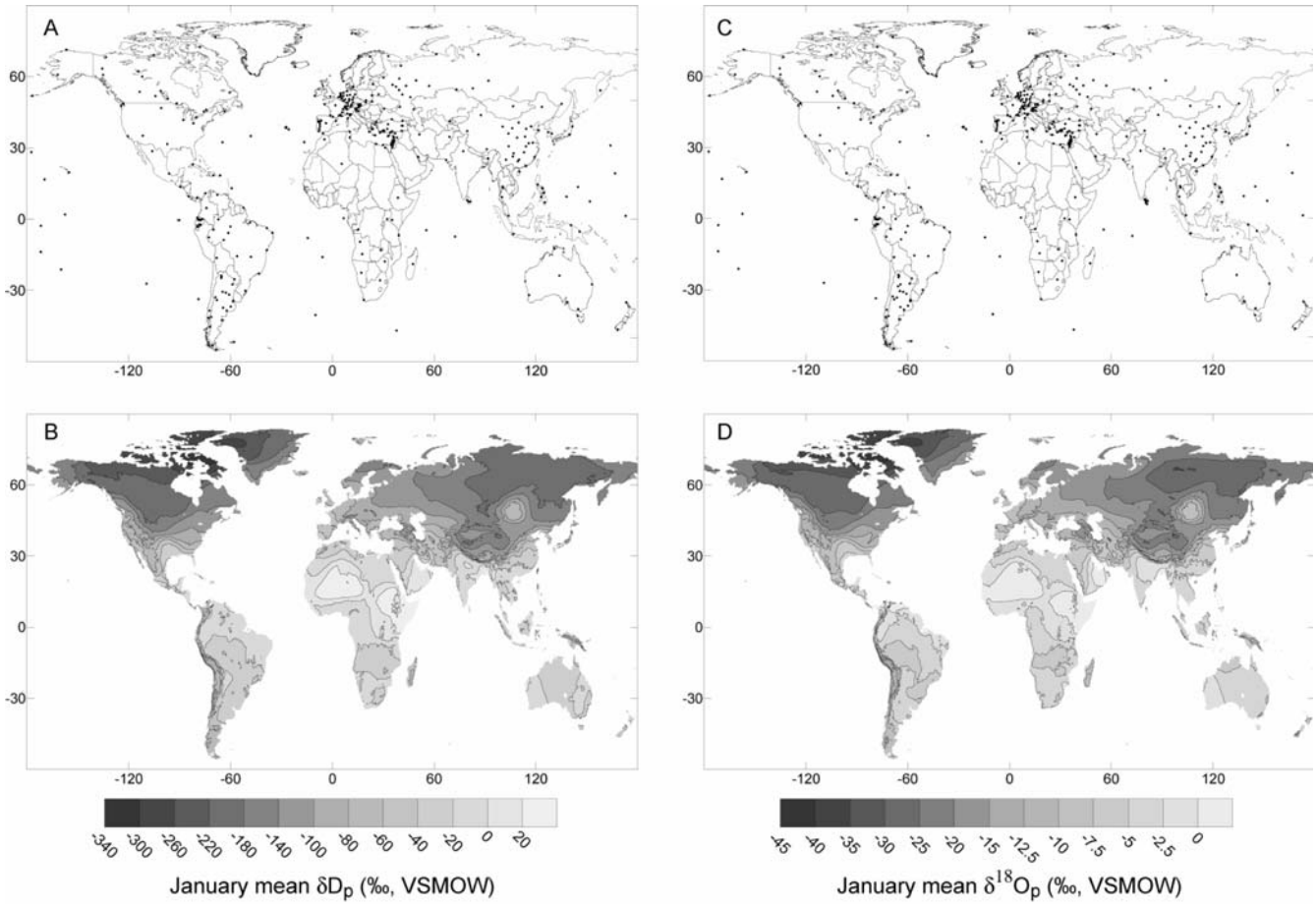

Fig. 1 Sampling station distributions (**a**, **c**, **e**, **g**) and interpolated isotope and climate grids (**b**, **d**, **f**, **h**) for the month of January. *Panels* represent δD_p (**a**, **b**), $\delta^{18}O_p$ (**c**, **d**), temperature (**e**, **f**) and precipitation amount (**g**, **h**)

Avian hydrogen isotope data

We compared feather hydrogen isotope (δD_f) measurements from North American (Hobson and Wassenaar 1997) and European (Hobson et al. 2004) data sets to our precipitation water isotope maps using regression analysis. In this analysis, it is important that both δD_f and δD_p values are subject to similar levels of natural variance and analytical uncertainty. For δD_p, this is a combination of uncertainty associated with collection and measurement of samples (typically $< \pm 2‰$) and with the interpolation model. Bowen and Revenaugh (2003) examined model uncertainty for interpolation of MA δD_p values and found it to be quite low (± 2–$6‰$) over much of the globe, but as high as $\pm 40‰$ in some high latitude regions. δD_f values, on the other hand, are subject to analytical uncertainty (typically $< \pm 2‰$), isotopic inhomogeneity within individual feathers, and intra-population variance. Sample inhomogeneity is still poorly understood, and could vary among species with different physiology and plumage characteristics. Our own experience suggests that intra-sample δD_f variance could range between $\pm 1‰$ and $\pm 5‰$. Intra-population variance may reflect physiological or behavioral variation among individuals or temporal variation in the δD of water sources, and is typically between $\pm 5‰$ and $\pm 15‰$ (e.g., Hobson and Wassenaar 1997). Because neither of the variables can be known exactly, standard *y*-on-*x* linear (standard ordinary least squares) regression is an inappropriate way of comparing feather and precipitation water isotope values. Here, we adopt reduced major axis (RMA) regression, which is appropriate when both variables are characterized by similar levels of uncertainty (Sokal and Rohlf 1995). The least squares estimator of the RMA regression slope is equal to square root of the ratio of variances of the two variables.

We regressed the δD_f data onto estimated site δD_p obtained from our grids. In addition to giving information on the relationship between feather and precipitation hydrogen isotopes, this regression provides a predictive model, or transfer function, that allowed us to transform our δD_p grids into "best predicted" δD_f values for the regions sampled in these feather data sets. To estimate the confidence of these predicted δD_f values, we calculated the standard deviation of regression model predictions (σ_f):

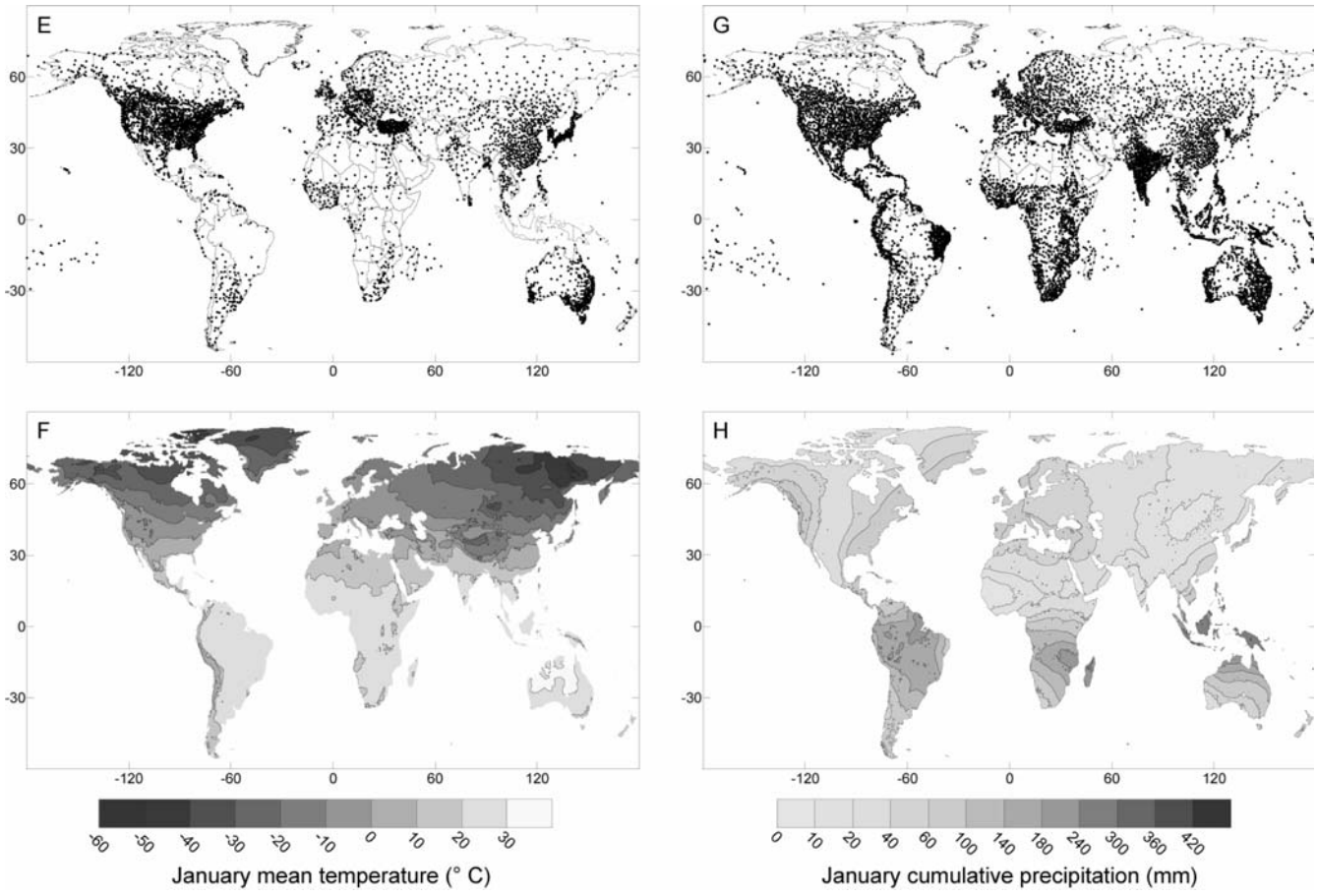

Fig. 1 (Contd.)

$$\sigma_f = \sqrt{\mathrm{MSE}_f \left(\frac{1}{m} + \frac{1}{n} + \frac{\left(\delta \mathrm{D_p} - \bar{\delta}_\mathrm{p}\right)^2}{\mathrm{VAR_p}} \right)}, \qquad (5)$$

where MSE_f is the mean square error for the regression model with respect to $\delta \mathrm{D_f}$, m is the number of observations in the 'unknown' data set, and n is the number of $\delta \mathrm{D_p}/\delta \mathrm{D_f}$ pairs, and $\bar{\delta}_\mathrm{p}$ and $\mathrm{VAR_p}$ are the average and variance of site $\delta \mathrm{D_p}$ values within the regression set (Sokal and Rohlf 1995). The standard deviations for each map grid cell were converted to 95% prediction intervals (PI) using the t-statistic, where the degrees of freedom were equal to $n-2$. Importantly, the power of the regression predictions increases with the number of observations made for the population of unknown origin (m). For some applications, such as the assignment of origin of a drug crop thought to originate in a single geographic region, it is reasonable to expect that m could be very large. In natural wildlife populations, however, the situation is more complicated. A single group of migratory birds, for example, is likely to include individuals having originated over a significant geographic range, making the relationship between sample population isotopic variance somewhat ambiguous. Further work and consideration of the characteristic ranges of specific bird populations will be necessary to define the statistical advantage gained by increasing sample numbers in wildlife migration studies (e.g., Rubenstein and Hobson 2004), and here, we consider only the simple case of assignment of the origin of a single individual, for which $m=1$. To check these analytical prediction intervals, we conducted cross-validation experiments, excluding each feather sample in turn and recalculating the regression model based the data from all other samples. The results of these experiments are reported as the percentage of samples for which the measured $\delta \mathrm{D_f}$ fell outside of the $\pm 95\%$ PI.

Results and discussion

Spatial distribution of growing-season $\delta \mathrm{D_p}$

Our interpolation methods produce continuous trend surfaces representing the major global and regional precipitation isotope, temperature, and precipitation amount monthly distributions (Fig. 1b, d, f, h). For water hydrogen and oxygen isotopes and monthly mean temperature, the strong zonal and altitudinal trends represented by the detrending model are evident. All the

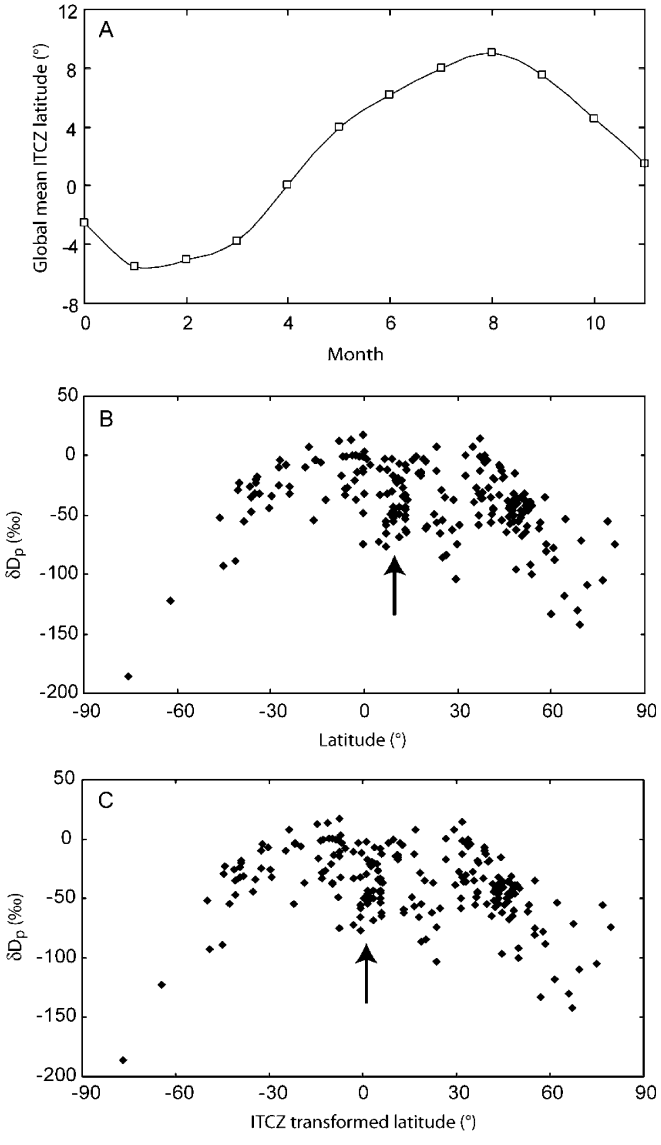

Fig. 2 Premise for transforming station latitudes based on the seasonal migration of the intertropical convergence zone (*ITCZ*). **a** Monthly, global average ITCZ latitude estimated from Waliser and Gautier (1993). **b** Untransformed δD_p data for July, illustrating the zonal asymmetry of the monthly isotope/latitude relationship. *Arrow* indicates the δD_p low associated with high precipitation amount in the ITCZ. **c** Transformed δD_p data for July, exhibiting a more symmetric zonal distribution and tropical δD_p low translated to near 0° transformed latitude (*arrow*)

maps also depict patterns of geospatial variation not directly related to these global trends, such as the relative dryness of the continental interiors (Fig. 1h) and meridional temperature gradients across northern Europe (Fig. 1f). Local to regional geospatial trends evident in the January precipitation isotope maps include meridional gradients across the Amazon Basin and northern Europe, enhanced depletion of the heavier isotopes through the North American cordillera and continental plain, and a region of anomalously high values in central Asia (Fig. 1b, d). In many cases, similarities between the isotope and climatological maps are indicative of the mechanisms driving geospatial water isotope variation. For example, the meridional isotopic pattern across northern Europe correlates well with decrease in temperature and precipitation amount from west to east, and reflects distillation of the heavy isotope from eastward-moving air masses as they cool and dry during their traverse across the continent. In central Asia, heavy isotope enrichment in January precipitation correlates with extreme seasonal dryness, and likely reflects the delivery of heavily evaporated water to the monitoring site at Ulan Bator and the surrounding regions.

The δD_p and $\delta^{18}O_p$ maps presented in Fig. 3 (a, c) represent the first global compilation of GS precipitation isotope data in a map form applicable to forensic studies. As was the case for the individual monthly grids, latitudinal, altitudinal, and regional patterns are depicted here. The heaviest GS δD_p and $\delta^{18}O_p$ values ($>0‰$ δD and $-2‰$ $\delta^{18}O$) were found in eastern and Saharan Africa and parts of the Arabian Peninsula. Heavy values are also found over other low-latitude regions such as equatorial and subtropical South America and southeast Asia. At the global scale, the most distinct patterns in GS precipitation isotope values are the zonal trends across North America, southern South America, and northeastern Asia, meridonal or oblique trends across Alaska and Eurasia, and the altitudinal trends over major mountain chains such as the Andes.

The overall geospatial pattern of GS precipitation isotope value is very similar to that of MA δD_p and $\delta^{18}O_p$ calculated from the same monthly water isotope and precipitation amount grids (Fig. 3b, d). Across most of the tropical and subtropical latitudes, as well as some coastal mid-latitude regions, the entire year is characterized by temperatures above 0°C and is part of the growing-season as defined here. For these regions the MA and GS fields are identical. The greatest differences between GS and MA values occur at the northern high latitudes, and can exceed 40‰ for δD_p and 6‰ for $\delta^{18}O_p$. In these regions, precipitation isotope values covary seasonally with temperature (Rozanski et al. 1993, Bowen (in preparation)), and the removal of wintertime values has a strong impact on the resulting seasonal δD_p and $\delta^{18}O_p$ estimates.

Each of the global and regional patterns evident in the maps of Fig. 3 could be useful for forensic studies at some scale, but these patterns provide the greatest power to trace the origin of biological samples when strong, unidirectional trends in water isotope values exist across broad regions. To provide an illustration of the potential and limitations of hydrogen isotope tracers in wildlife forensic and migration studies, we examined the spatial GS δD_p variation across four continental regions. In many ways, North America provides an ideal setting for forensic isotope studies, with a strong, simple, zonal gradient of 130‰ characterizing much of the continent (Fig. 4). Some complexity is added to this pattern due to the topography of the Western cordillera, but local

altitudinal variation is generally small in comparison to the overall zonal trend. Substantial isotopic gradients also exist from the west coast inland, and in cases where the range of a species of interest spans the cordillera, the similarity of isotopic values on the west and east side of this feature will reduce the power of the water isotope tracer method. The δD_p gradient across Europe is somewhat smaller than that of North America, with a total range of ~100‰ from the Mediterranean coastal regions to northern Scandinavia (Fig. 5). The strongest GS δD_p gradients exist across western Europe and in Scandinavia, suggesting that there is good potential for using water isotopes to constrain the origin of wildlife samples from these regions. Across large regions of central Europe, however, δD_p is almost invariant, and δD_p low associated with the Alps make up the most significant isotopic relief. It is unlikely that the δD and $\delta^{18}O$ tracer method could successfully resolve the origin of most materials within central Europe, but clearly potential does exists for the forensic assignment of samples within some regions, including Iberia, western Europe, and Scandinavia.

The spatial distribution of δD_p across two tropical and subtropical regions demonstrates the limitations of the water isotope forensic tracer method over many low latitude regions. There is some variation in δD_p across Northern Africa (Fig. 6), the primary features of which are a strong δD_p maximum over the horn of East Africa and heavy isotope enrichment in precipitation over the Sahara. The Arabian Peninsula displays a simpler pattern of GS δD_p variation, with a monotonic decrease in isotope values occurring from the southeast to the northwest. Values are somewhat lower across the southern part of the African continent, but the total range of δD_p values for this continent is of the order of 40‰. Because of a limited water isotope range, the application of the hydrogen isotope tracer method for African samples will be strongly dependent on the quality of the relationship between wildlife samples and environmental water, with weak relationships severely compromising forensic applications.

The case of Amazonian South America is somewhat different. The total range of GS δD_p values east of the Andes and north of Argentina is only ~30‰, wholly insufficient to allow assignment of samples except under the most ideal circumstances. The primary isotope structure in northern South American δD_p is a dramatic low over the Andes, where estimated δD_p gradients of as

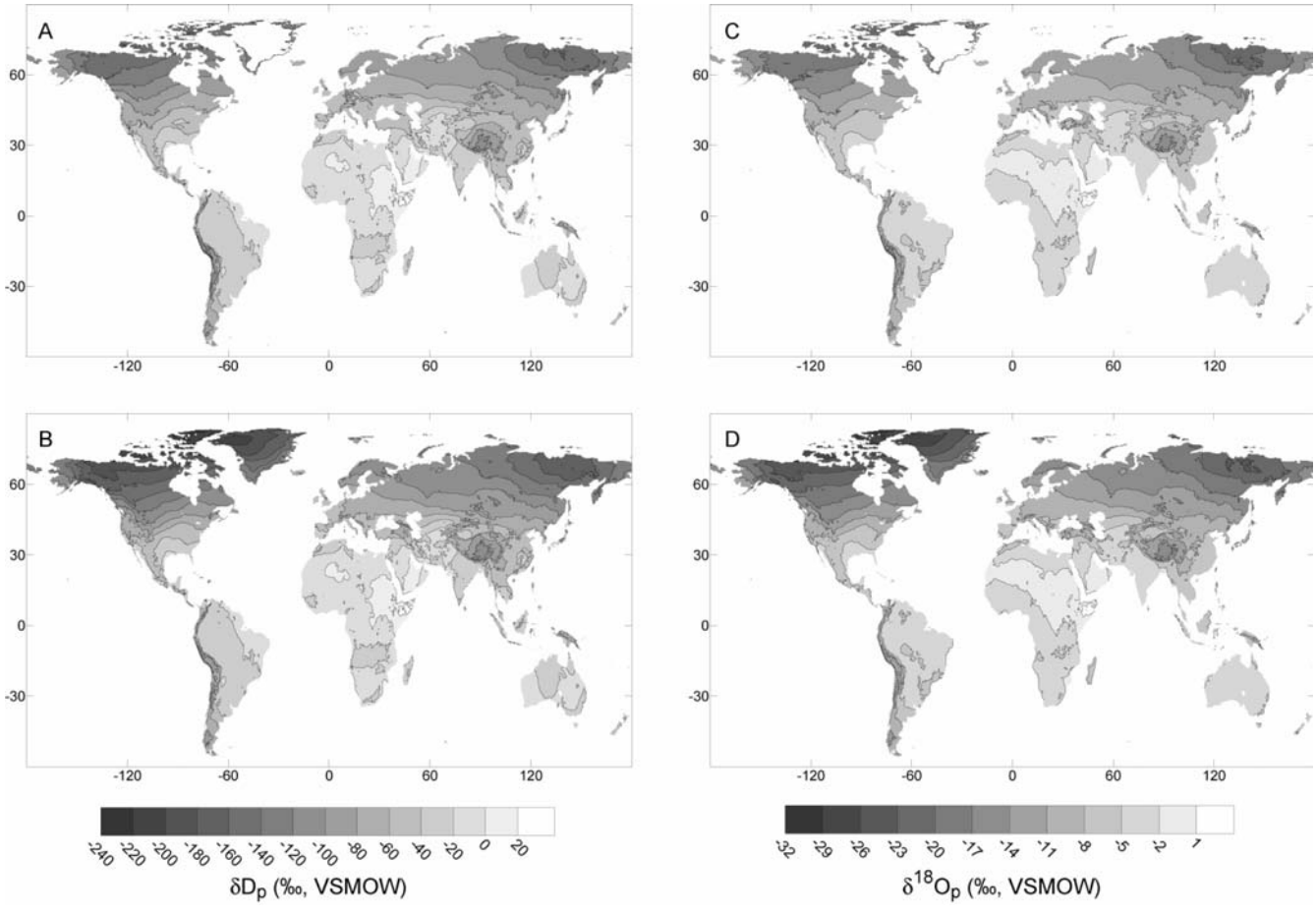

Fig. 3 Interpolated growing-season (**a**, **c**) and mean annual (**b**, **d**) global maps for δD_p (**a**, **b**) and $\delta^{18}O_p$ (**c**, **d**). Growing-season and mean annual values are plotted on the same scale. For hatched

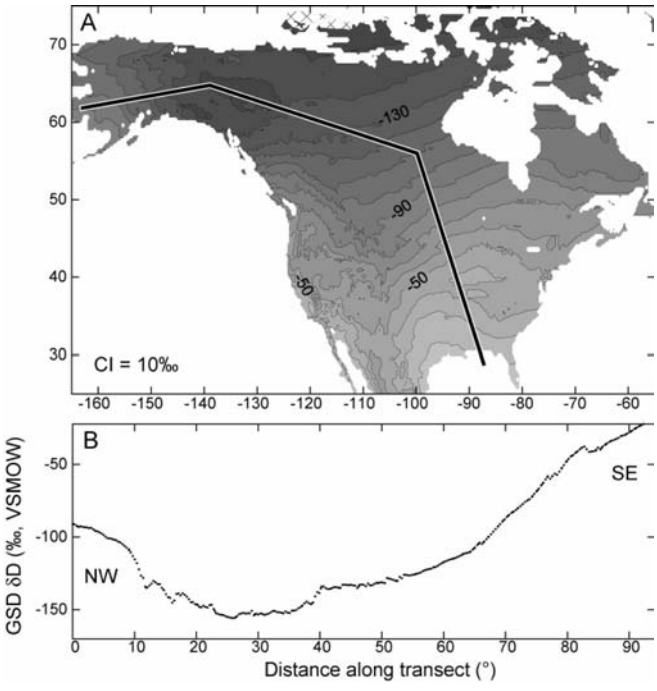

Fig. 4 Map (**a**) and profile (**b**) of growing-season (*GS*) δD_p for North America. Line of profile is shown in **a**, and the northwest (*NW*) and southeast (*SE*) ends of the profile indicated in **b**. *CI* Contour interval. For hatched areas in **a**, no month met the criterion for a growing-season month. Profile *lines* here and in Fig. 5, 6, 7 are subjectively chosen transects shown to illustrate the major features of each region's geospatial water isotope distribution

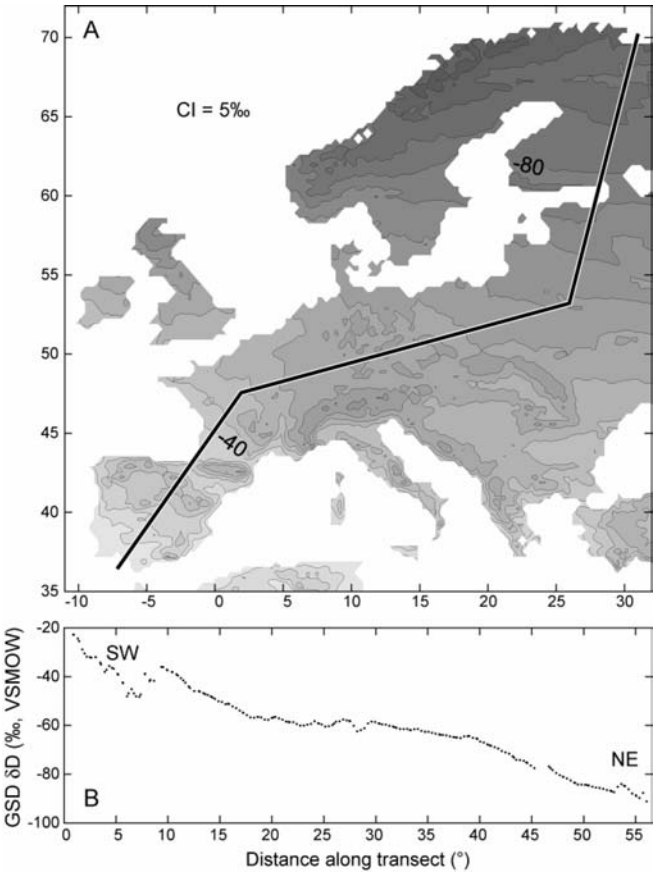

Fig. 5 Map (**a**) and profile (**b**) of GS δD_p for Europe. *Line* of profile is shown in **a**, and the northeast (*NE*) and southwest (*SW*) ends of the profile indicated in **b**. *CI* Contour interval

much as 70‰ exist over short distances. The main promise of the water isotope tracer application in northern South America, then, may be its application to distinguish between high- and low-altitude source areas (e.g., Hobson et al. 2003). Additional potential exists in the southernmost part of the continent, where a strong north to south decrease in δD_p exists.

The relationship between δD_p and δD_f

There is strong relationship between individual feather δD values from both Europe and North America and collecting site GS or MAD δD_p (Fig. 8). The coefficient of determination for the $\delta D_f/\delta D_p$ regression is similar for the GS and MAD regressions on each continent, but is somewhat larger for the North America than for Europe (0.85–0.86 vs. 0.65–0.67). The North American samples span a much greater range of δD_f and δD_p values than do the European samples, and are more evenly distributed throughout that range.

The ideal, unmodified incorporation of the precipitation isotope signal into feathers would result in a regression line with a slope of 1, and deviations from this relation indicate modification of the precipitation isotope signal by physical or biological processes during its transfer from precipitation to diet and ultimately to feathers. The slopes of all four regressions are close to 1, but significant differences exist between the two continents and the two δD_p grids. The North American data set was published prior to development of routine corrections for a ~10% δD bias due to the presence of hydrogen in feather keratin that freely exchanges with hydrogen in atmospheric water vapor (Schimmelmann 1991; Wassenaar and Hobson 2000). In order to make the North American and European regression slopes more directly comparable, we calculated an adjusted slope for the North American cases by multiplying the raw regression slope by 1.10. These adjusted slopes are similar to the slopes for the European data, which include corrections for hydrogen exchange (Wassenaar and Hobson 2002), although the upper 95% CI for the transformed North American δD_f/GS δD_p regression slope (1.13) still does not overlap the lower CI for the equivalent European regression (1.14).

For each feather data set, the (adjusted) slope of the GS regression is >1 and the MAD regression is <1, suggesting that the δD signal incorporated into feathers may be intermediate to GS and MA values. This could arise from the uptake of non GS (winter moisture) or stored soil water by plants (Ehleringer and Dawson 1992). Alternatively, biophysical processes may systematically amplify the GS δD_p signal in the foodweb. One

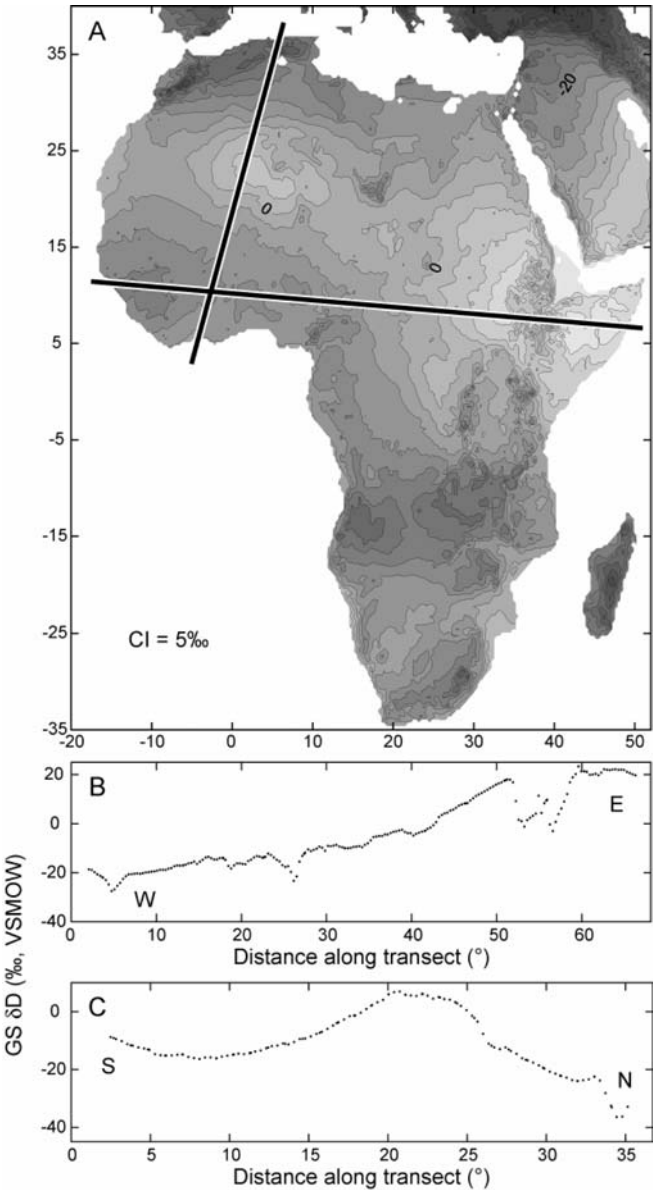

Fig. 6 Map (**a**) and two profiles (**b**, **c**) of GS δD_p for North Africa. *Lines* of profile are shown in (**a**), and the north (*N*) and south (*S*) or west (*W*) and east (*E*) ends of the profiles indicated in **b** and **c**. *CI* Contour interval

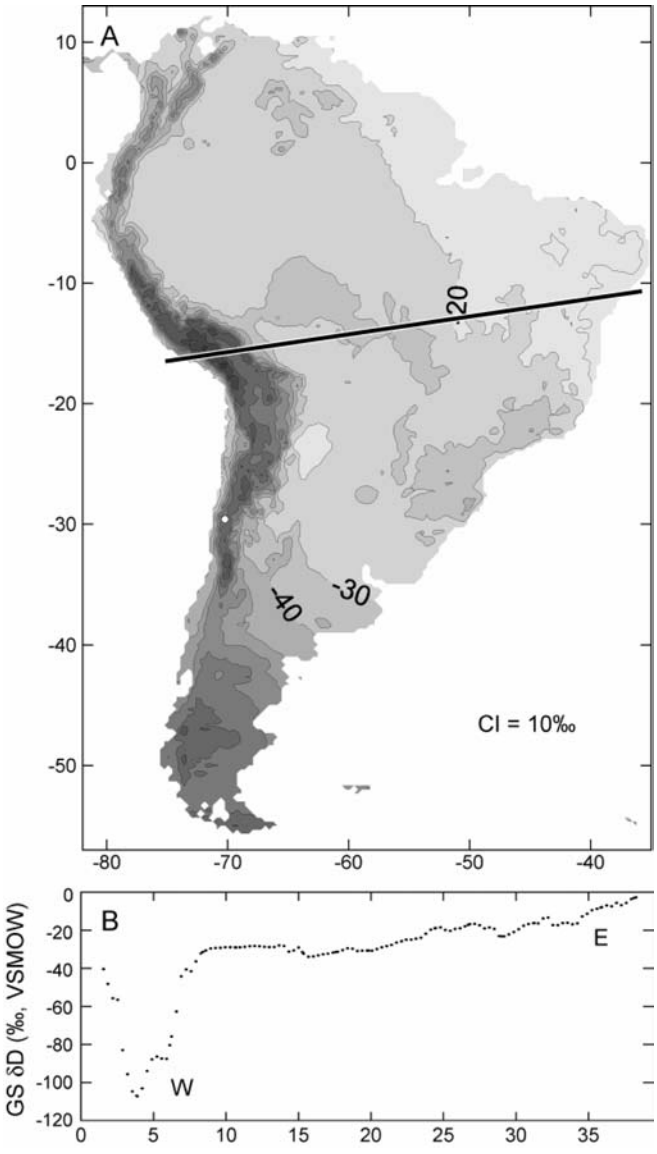

Fig. 7 Map (**a**) and profile (**b**) of GS δD_p for South America. *Line* of profile is shown in **a**, and the west (*W*) and east (*E*) ends of the profile indicated in **b**. *CI* Contour interval

possible mechanism is enhanced evaporative enrichment of plant water (Flanagan et al. 1991) in warmer regions characterized by higher δD_p. Whatever the case, it is apparent that spatial variation in GS δD_p is not directly transferred to feathers in a simple 1:1 fashion, but is modified in some currently unknown and systematic way.

The intercept of δD_f/GS δD_p has been described as a net "fractionation factor" that accounts for the offset between δD_f and δD_p values (e.g., Hobson and Wassenaar 2001). In reality, this parameter represents the effects of a variety of still undetermined physical and biophysical processes, and may not be constant for all species or habitats (e.g., Lott et al. 2003). Our reanalysis of the North American and European feather δD_f data sets shows the regression line intercept to be variable, particularly so for the two regressions of the European data (also see Hobson et al. 2004). Because exchangeable hydrogen corrections have not been applied to the North American samples, the intercepts for those regressions can not be compared directly with the ones based on the European data set, but the intercept for δD_f in the North American regressions does appear less sensitive to the choice of precipitation grid than that for the European regressions. Until a more complete understanding of the isotope effects and fractionation involved in the transfer of δD_p to feather keratin (and other biological substrates of interest) is developed, the $\delta D_f/\delta D_p$ relationship will need to be investigated on a case-by-case basis and application of

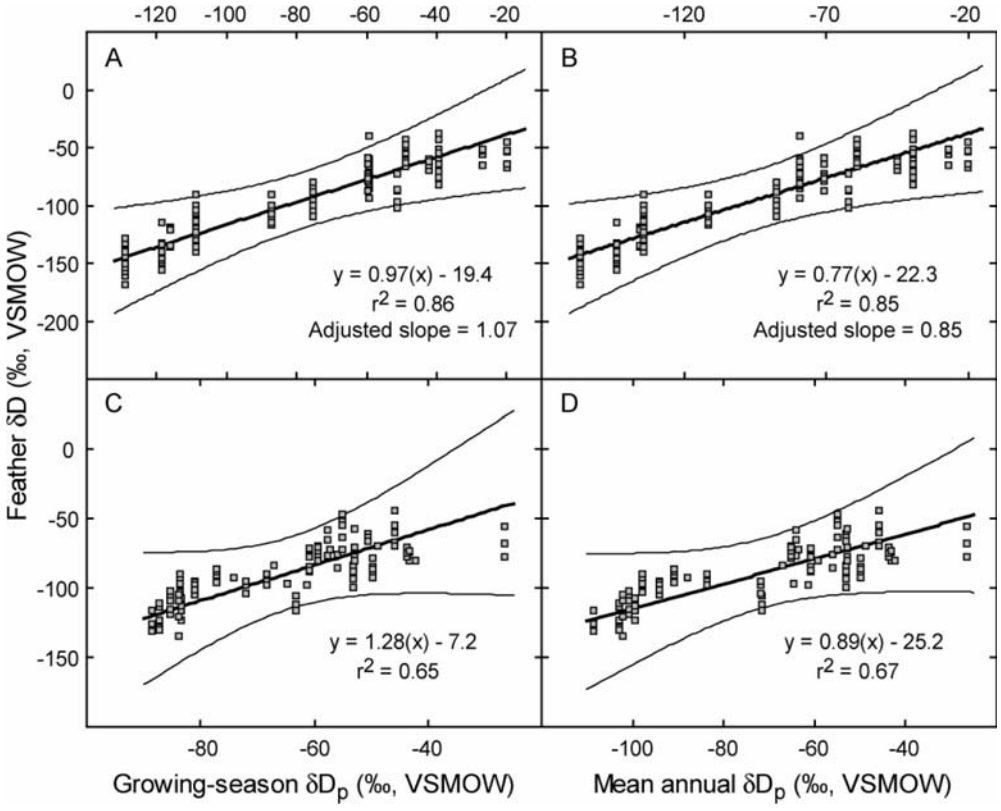

Fig. 8 Regression of North American feather δD data from (Hobson and Wassenaar 1997) against growing-season δD_p (**a**) and mean annual δD_p (**b**), and of European feather δD data (Hobson et al. 2004) against growing-season δD_p (**c**) and mean annual δD_p (**d**). Equations for the best-fit lines and coefficient of determination are given for each regression. Adjusted slope in **a** and **b** indicates the regression slope following correction for exchangeable hydrogen, as described in the text

a generic fractionation factor relating these parameters is strongly discouraged.

Wildlife forensic applications using δD_p grids

We used the regression relationships between the two δD_f data sets and our δD_p grids, to illustrate how the water isotope grids can be used in forensic applications to determine the origin of unknown samples. The equations for the regression lines yield regional transfer functions that can be used to convert the δD_p gridpoint values to estimates of the mean δD_f for birds originating at locations across the grid. An estimate of confidence for the mean δD_f values is given by the upper and lower 95% PIs for the $\delta D_f/\delta D_p$ regressions (Fig. 8). These prediction intervals incorporate all sources of error contributing to uncertainty in the δD_f predictions, including intra- and inter-sample variability and possible errors in the interpolated δD_p fields, and should therefore yield a robust estimate of the confidence of the transfer function. In our cross-validation experiments, only 1.8% of North American feather samples had δD values that fell outside the 95% PIs for their location. For Europe, the percentage was 1.6% for the GS δD_p regression and 0.8% for MA δD_p, confirming that the reported analytical PIs meet or exceed the quoted levels of confidence. The width of the prediction envelops shown in Fig. 8 is closely tied to the strength of the regressions. For the North American cases there was no overlap of the 95% prediction envelopes at the high and low ends of the δD_p range, and the hydrogen isotope tracer method has much greater predictive power than in Europe, where overlap is present throughout the δD_p range.

Using the transfer functions and PIs for the North American and European avifauna data sets and the GS δD_p grid, we delineate 95% confidence zones in North America and Europe for the origin of three hypothetical feather samples having measured δD values of -150, -100 and -50‰. On each continent, the transfer functions clearly constrain the origins of the -150‰ and -50‰ samples to non-overlapping zones, whereas the origin of the sample with intermediate δD is constrained to within a zone that overlaps those for the light and heavy samples to some extent. An obvious difference between the reconstructions for the two continents is that the European transfer function has no power to constrain the zone of origin for the intermediate feather sample on that continent, whereas in North America some 50% of the continent lies outside of the 95% confidence zone for the sample's origin. Both the stronger correlation of δD_f and δD_p for the North American feather data set and the wider range of δD_p

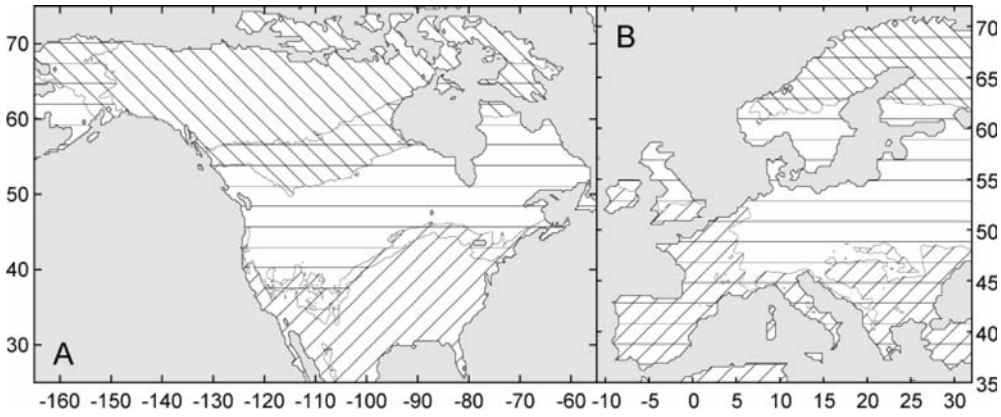

Fig. 9 Zones of 95% confidence for the predicted origin of feather samples with δD values of −150% (hatching oriented to northwest), −100% (horizontal hatching), and −50% (hatching to northeast) based on the growing-season regression models for North America (**a**) and Europe (**b**)

values for the North American continent contribute to this difference. Although the zones illustrated in Fig. 9 are plotted across the entire map area, we caution that the observed variability in the $\delta D_f/\delta D_p$ regressions implies that this method should not be used to estimate origins of samples that may have come from geographic regions lying well outside the coverage of the training set. On the other hand, for most real-world applications the broad zones plotted in Fig. 9 can be considerably narrowed by drawing on the known ranges of the species of interest. In practice, therefore, forensic application of isotopes will be more powerful when basic data concerning geographic range and distribution of the species are considered.

Additional factors may considerably increase the power of this method in future work. The δD_f data sets used here include feather samples from a large number and diversity of taxa, and it is possible that variation in the suite of physical and biophysical factors controlling the δD offset between water and feathers of these different taxa decreases the strength of the predictive regressions. Although preliminary findings suggest that the water/feather fractionation factor is relatively insensitive to trophic level, differences have been observed for different of types habitat (Lott et al. 2003) and additional work will be needed to determine the degree to which feeding strategy and habitat type affects this relationship. Such factors could be described through taxonomically-specific regression models, but perhaps a more exciting direction for this work would be the development of generalized predictive models for the isotopic composition of plant and animal tissues that incorporate the effects of environmental, behavioral, and physiological variables. Studies are being conducted that could form the groundwork for such a model (e.g., McKechnie et al. 2004), but many unknowns remain.

The example provided here applies to the most general case in which we seek to constrain the origin of an individual specimen with no a priori knowledge of the population from which it was derived. Additional predictive power could be developed if population statistics and statistical assignment methods were applied to the reconstruction of the origin of suites of samples from groups of individuals known to migrate together. Lastly, the power of the isotope method may be significantly improved in cases where it can be combined with other isotopic tracers and chemical assays that vary systematically over geographic scales (Hobson 2003).

Conclusions

Global GS precipitation isotope grids presented here provide a foundation for future wildlife and criminal forensic applications involving stable hydrogen and oxygen isotopes. The grids provide the fundamental geospatial patterns for the underlying precipitation source signal, and thus serve as a guide to potential forensic applications around the globe. A number of regions show great promise, and existing feather isotope data sets from these regions reveal that a strong relationship between animal tissues and δD_p exists and has the power to statistically constrain the origin of unknown samples. Uncertainties remain regarding the parameters that relate tissue isotope values to δD_p and $\delta^{18}O_p$ and the degree to which they are constant among species and habitats, yet given the diversity and complexity of the processes linking precipitation and animal tissues, the strength and general similarity of the observed relationships are very encouraging. Further deciphering isotopic fractionation among local hydrological and food web components and modeling these effects at regional or continental scales represents a fundamental area of research that could lead to robust and powerful forensic application of the water isotope tracer method worldwide. Until further understanding of those processes has been developed, however, studies that seek to apply isotope tracers in a statistical predictive sense should include calibration data derived

from samples of known origin. Even where such data can not be gathered, stable isotope measurements have the potential to provide insight into animal behavior and population ecology, and further isotopic studies of natural populations are encouraged.

Acknowledgements This work was supported in part by Contract IS-FO-2029 from the Technical Science Working Group to TE Cerling and JR Ehleringer. Additional funding was provided by operating grants from Environment Canada to KAH and LIW.

References

Ayliffe LK et al (2004) Turnover of carbon isotopes in tail hair and breath CO_2 of horses fed an isotopically varied diet. Oecologia 139:11–22

Bowen GJ, Revenaugh J (2003) Interpolating the isotopic composition of modern meteoric precipitation. Water Resources Research 39, 1299. DOI 10.129/2003WR002086

Bowen GJ, Wilkinson B (2002) Spatial distribution of $\delta^{18}O$ in meteoric precipitation. Geology 30:315–318

Chamberlain CP, Blum JD, Holmes RT, Feng XH, Sherry TW, Graves GR (1997) The use of isotope tracers for identifying populations of migratory birds. Oecologia 109:132–141

Craig H (1961) Isotopic variations in meteoric waters. Science 133:1702–1703

Dansgaard W (1954) The O^{18}-abundance in fresh water. Geochim Cosmochim Acta 6:241–260

Dansgaard W (1964) Stable isotopes in precipitation. Tellus 16:436–468

Ehleringer JR, Dawson TE (1992) Water uptake by plants: perspectives from stable isotope composition. Plant Cell Environ 15:1073–1082

Estep MF, Dabrowski H (1980) Tracing food webs with stable hydrogen isotopes. Science 209:1537–1538

Evans-Ogden LJ, Hobson KA, Lank DB (2004) Blood isotopic ($\delta^{13}C$ and $\delta^{15}N$) turnover and diet-tissue fractionation factors in captive Dunlin. Auk 121:170–177

Flanagan LB, Bain JF, Ehleringer JR (1991) Stable oxygen and hydrogen isotope composition of leaf water in C_3 and C_4 plant species under field conditions. Oecologia 88:394–400

Gat JR, Bowser CJ, Kendall C (1994) The contribution of evaporation from the Great Lakes to the continental atmosphere; estimate based on stable isotope data. Geophys Res Lett 21:557–560

Hobson KA (1999) Tracing origins and migration of wildlife using stable isotopes: a review. Oecologia 120:314–326

Hobson KA (2003) Making migratory connections with stable isotopes. In: Berthold P, Gwinner P (eds) Avian migration. Springer, Berlin Heidelberg New York, pp 379–391

Hobson KA, Clark RG (1992) Assessing avian diets using stable isotopes, 1. Turnover of C-13 in tissues. Condor 94:181–188

Hobson KA, Wassenaar LI (1997) Linking breeding and wintering grounds of neotropical migrant songbirds using stable hydrogen isotopic analysis of feathers. Oecologia 109:142–148

Hobson KA, Wassenaar LI (2001) Isotopic delineation of North American migratory wildlife populations: loggerhead shrikes. Ecol Appl 11:1545–1553

Hobson KA, Atwell L, Wassenaar LI (1999) Influence of drinking water and diet on the stable-hydrogen isotope ratios of animal tissues. Proc Nat Acad Sci USA 96:8003–8006

Hobson KA, Wassenaar LI, Mila B, Lovette I, Dingle C, Smith TB (2003) Stable isotope as indicators of altitudinal distributions and movements in an Ecuadorean hummingbird community. Oecologia 136:302–308

Hobson KA, Bowen GJ, Wassenaar LI, Ferrand Y, Lormee H (2004) Using stable hydrogen and oxygen isotope measurements of feathers to infer geographical origins of migrating European birds. Oecologia 141:477–488

IAEA/WMO (2001) Global network for isotopes in precipitation, the GNIP database

Kendall C, Coplen TB (2001) Distribution of oxygen-18 and deuterium in river waters across the United States. Hydrol Process 15:1363–1393

Lott CA, Meehan TD, Heath JA (2003) Estimating the latitudinal origins of migratory birds using hydrogen and sulfur stable isotopes in feathers: influence of marine prey base. Oecologia 134:505–510

McKechnie AE, Wolf BO, del Rio CM (2004) Deuterium stable isotope ratios as tracers of water resource use: an experimental test with rock doves. Oecologia 140:191–200

Meehan TD et al (2001) Using hydrogen isotope geochemistry to estimate the natal latitudes of immature Cooper's hawks migrating through the Florida Keys. Condor 103:11–20

Norris DR, Marra PP, Kyser TK, Sherry TW, Ratcliffe LM (2003) Tropical winter habitat limits reproductive sucess on the temperate breeding grounds in a migratory bird. Proc R Soc Lond Ser B 271:59–64

Peterson TC, Vose RS (1997) An overview of the global historical climatology network temperature data base. Bull Am Meteorol Soc 78:2837–2849

Rozanski K, Araguas-Araguas L, Gonfiantini R (1993) Isotopic patterns in modern global precipitation. In: Swart PK, Lohmann KC, McKenzie J, Savin S (eds) Climate change in continental isotopic records. American Geophysical Union, Washington DC, pp 1–36

Linking breeding and wintering ranges of a migratory songbird using stable isotopes. Science 295:1062-1065

Rubenstein DR, Hobson KA (2004) From birds to butterflies: animal movement patterns and stable isotopes. Trends Ecol Evol 19:256-263

Schimmelmann A (1991) Determination of the concentration and stable isotopic composition of nonexchangeable hydrogen in organic matter. Anal Chem 63:2456–2459

Sokal RR, Rohlf SJ (1995) Biometry: the principals and practice of statistics in biological reserach, 3rd edn. (WH) Freeman, New York

US National Geophysical Data Center (1998) ETOPO-5 five minute gridded world elevation. In: NGDC, Boulder, Colorado, USA

Waliser DE, Gautier C (1993) A satellite-derived climatology of the ITCZ. J Climate 6:2162–2174

Wassenaar LI, Hobson KA (1998) Natal origins of migratory monarch butterflies at wintering colonies in Mexico: new isotopic evidence. Proc Nat Acad Sci 95:15436–15439

Wassenaar LI, Hobson KA (2000) Improved method for determining the stable-hydrogen isotopic compositon (δD) of complex organic materials of environmental interest. Environ Sci Tech 34:2354–2360

Wassenaar LI, Hobson KA (2002) Comparative equilibration and online technique for determination of non-exchangeable hydrogen of keratins for use in animal migration studies. Isotope Environ Health Stud 39:1–7

Webster MS, Marra PP, Haig SM, Bensch S, Holmes RT (2001) Links between worlds: unraveling migratory connectivity. Trend Ecol Evol 17:76–83